11^{th} International Conference on Fracture Mechanics of Concrete and Concrete Structures
FraMCoS-11
J. M. Chandra Kishen, A. Ramaswamy, S. Ray and R. Vidyasagar (Eds)
https://doi.org/10.21012/FC11.0923106

STUDY OF SCALED FRACTURE PARAMETERS IN CONCRETE USING FINITE SIMILITUDE THEORY

MANSI GUPTA[*1], **SONALI BHOWMIK**[*2]

[*]Department of Civil Engineering
National Institute of Technology Rourkela, Odisha, India
e-mail[1]: 521ce1012@nitrkl.ac.in
e-mail[2]: bhowmiksonali@nitrkl.ac.in

Key words: Finite Similitude Theory, Concrete, Stress Intensity Factor, Scaling

Abstract. The study of fracture is presently based on the dimensional analysis theory which assumes the invariance of dimensionless equations with scale. However, in reality, the dimensionless equations also change with scaled experimentation. The application of dimensional analysis to very large structures is limited due to presence of significant scaling ratios and size effect. To overcome these limitations of dimensional analysis, the fracture parameters are reanalyzed using a new scaling theory called finite similitude theory. The concept of finite similitude is based on the metaphysical notion of space scaling, where changes during the space and time deformation are assessed in view of physical and trial space. This concept can be applied to all physics and is able to quantify the scale dependencies more precisely. It has been applied to various domains such as impact mechanics, powder compaction, biomechanics, electromagnetism and proved reliable in formulating the scale dependencies accurately. Till now, this concept has been explored in the domain of linear elastic fracture mechanics and elastic-plastic fracture mechanics. Here the concepts of finite similitude have been explored for notched concrete beam specimens under three-point bending tests. The fracture parameter (stress intensity factor (K_I)) is defined under quasistatic loading using first-order similitude theory. Finite element analysis has been performed to validate the applicability of proposed theory. The study highlights the appositeness of new finite similitude theory on the study of fracture parameters.

1 INTRODUCTION

Structural materials consist of various flaws, defects, or voids in their microstructure, which is virtually unavoidable. These flaws or defects, under the action of load, give rise to stress concentration zones and assist in the failure of material. Fracture mechanics is the field of solid mechanics that considers the presence of cracks in material and concerns with the propagation of these cracks under various loading conditions. It is based on the twin pillars of analytical and experimental mechanics for the quantification and characterisation of crack driving force and resistance offered by the material. Fracture mechanics, in its simplest form, is a method for predicting failure for loaded components with inherent flaws. It also offers the correct definition for classifying cracks into those that propagate and those that do not. However, the scale dependence of material properties poses a major challenge in the accurate prediction of structural failure. Leonardo da Vinci [1], in his experiments on load bearing capacity of iron wires stated that "Among the cords of equal thickness, the longest wire is the one with least strength". This phenomenon was termed as "scale effect". Galileo [2] further extended this study and declared that the decrease in dimension of struc-

ture increases its strength. The primary issue associated with scaling pertains to scale effects, wherein the behaviour of the scaled system notably differs from that of the system at its full size. If the scale effect is absent, then the behaviour of full-scale system can be readily explained from the laboratory scale experiments. However, in reality, almost all the materials suffer from scale effect which generates the need for different studies considering the scale effect.

Regardless of the existence of scale effects, scaled experiments are carried out in industry. There are various reasons behind this, but the majority of them are related to the high expense and/or impracticability of full-scale studies. The concept of scaling finds extensive application across various domains of engineering, such as structural and fracture mechanics [3-4], structural impact [5], explosive engineering [6], and thermofluids [7]. The increased precision and efficacy of computer modelling has surely had an impact on the kind and nature of experiments conducted. A robust computational model has the potential to completely substitute trials, while also serving as a valuable complement to scaled experimentation. To some extent, modern numerical approaches can reduce the requirement of time and resource associated with large scale laboratory experimentations. The extended finite element method (XFEM) is a particularly useful example of a current approach for modelling and analysing crack growth. It was developed by Moes et al. [8], based on the notion of "partition of unity" and uses the enrichment functions around the crack tip. The enrichment function includes crack-tip asymptotic function for stress singularity around the crack tip and discontinuous function for displacement jump along the crack surface. The use of these functions enhance the analysis of stress and displacement fields in the vicinity of crack tip, thereby reducing the need for mesh refinement. The traction-separation cohesive behaviour is commonly employed in the XFEM framework within the Abaqus/Standard software [9] to simulate the initiation and propagation of cracks. However, in the context of intricate systems characterised by substantial uncertainties, it is not recommended to excessively depend on computational methods, therefore necessitating the presence of experiments. There are many scenarios where continuous monitoring is not feasible and hence the theoretical development of experimental data is necessary. Hence, experimentation and simulations must work side by side for developing a generalised theoretical model and providing a clear insight of scale and size effect.

The fracture behaviour of concrete is well-known for exhibiting size effects. The Weibull's statistical size effect theory [10] describes the size effect based on random strength of material. According to this theory, the larger structure has more probability of failure owing to larger chance of encountering a weaker strength value. However, it was later shown that this theory cannot be used to explain the behaviour of quasi-brittle materials that fail with larger cracks. Furthermore, when the structural size is relatively large and material is highly heterogeneous, the Weibull's statistical size effect theory cannot be used [4]. In contrast to the statistical size effect, Bazant [11] introduced the concept of the energetic size effect, which is based on deterministic energetic factors that contribute to the observed size effect. In simpler terms, it primarily takes into account the link between nominal stress and the material's characteristic size. Additionally, when both stress (strain) and energy are included in the fracture criterion, the scaling law provides a progressive transition from strength theory for small size to LEFM for large size. Bazant [12] used dimensional analysis approach to further explore the fracture and size effect in concrete. Crack growth rate under fatigue has been explored by various researchers using the concept of incomplete self-similarity and dimensional analysis [13-14].

Recently, a new scaling theory named finite similitude theory [15] has been appeared in open literature which describes all scale dependencies for a physical system without involving any approximation. Finite similitude theory

is based on the metaphysical concept of space scaling. The notion of manipulating the spatial dimensions to facilitate scaled experimentation appears to lack practicality. However, it is feasible to evaluate the influence of this metaphysical approach on the fundamental physics governing the behaviour of an experiment. Studies on application of similitude can be dated back to report submitted by Goodier and Thomson's [16] for the US Aeronautical Advisory Committee. Following this, Goodier's book [17] describing the applicability of similitude to structural systems was published in 1950. Davey et al. [18] introduced a new approach for scaled experimentation in fracture mechanics using finite similitude theory. This paper presents numerical simulations that illustrates the practical advantages of the newly proposed scaling theory in the field of fracture mechanics, particularly in situations where scale effects are prominent. The study was further explored for the utilisation of two experiment theory to predict the behaviour of large scale experiments by the same authors [19]. The finite similitude theory has the ability to connect more than one experiment. The first-order rule is used to incorporate results from two scaled models at different scales in order to predict the response behaviour of a prototype. The application of finite similitude has been extended to the scaled cohesive zone models for the fatigue crack propagations in metals [20]. It was shown that first order similitude theory can accurately reproduce the full scale behaviour of large structures. An overall review on the application of this theory on different engineering domains is reported by Davey et al. [21]. Till now, the applicability of finite similitude theory has been explored in the domain of linear elastic fracture mechanics and elastic-plastic fracture mechanics for the metals and alloys. In recent work by Davey et al. [22], it was shown via case studies that this theory can also be used for concrete. However, no extensive work can be found on application of first-order finite similitude theory for fracture properties of concrete.

In this study, an attempt has been made to study the application of finite similitude theory on fracture behaviour of concrete. The aim of this study is to assess the behaviour of a specimen across various scales based on the outcomes of two experiments conducted at selected scales. Here the concepts of finite similitude have been explored for notched concrete beam specimens under three-point bending tests. The stress intensity factor (K_I) is defined under quasi-static loading using first order similitude theory. For the crack growth modelling, XFEM has been performed in ABAQUS. The stress intensity factor is calculated in the ABAQUS software using contour integral method to validate the applicability of the proposed theory. The study demonstrates the significance of the first-order finite similitude condition in the context of fracture mechanics of concrete structures.

2 FINITE SIMILITITUDE THEORY

Finite similitude theory is based on the metaphysical concept of space scaling. This concept involves the contraction or expansion of space for the purpose of conducting scaled experiments. It is important to note that space scaling, although integral to the approach, cannot be physically realised. However, it is possible to evaluate the influence of scaling in the spatial domain on the physical limitations that govern the response of a structure.

2.1 Metaphysical concept of space scaling

Space-scaling is defined as a temporally invariant affine map denoted as $x_{ps} \leftarrow\!\shortmid\, x_{ts}$ that establishes a connection between coordinate points in two inertial frames. There is a frame located in the physical space (ps) and another frame situated in the trial space (ts). Both physical space and trial space are physical entities where various processes occur. In physical space, full-scale activities are carried out, whereas in trial space, scaled experimentation is conducted. The differential expression for the affine map can be written as $\boldsymbol{dx}_{ts} = \boldsymbol{F}\boldsymbol{dx}_{ps}$, where the matrix F remains invariant both in time and space. This expression relates coordinate functions and has the form $dx^i_{ts} = F^i_j dx^j_{ps}$,

where $F^i_j = dx^i_{ts}/dx^j_{ps}$, and x^i_{ts} and x^j_{ps} represent the coordinate functions for their respective inertial frames. At this initial phase of explaining the space-scaling approach, two advantages become apparent. Firstly, in contrast to dimensional analysis, the process offers a physical intuitiveness. Secondly, the form of F determines the nature of scaling, whether it is isotropic or anisotropic. The study here is limited to isotropic scaling only where F= βI, or in terms of coefficient $F^i_j = \beta\delta^i_j$, where δ^i_j is Kronecker delta symbol. The scalar β represents a positive real number that serves to quantify the degree of length scaling that is present. The space undergoes contraction for values of β between 0 and 1, where β = 1 represents no change in length. Space expansion is indicated by values of β greater than 1. Hence, this theory allows for both expansion and contraction of physical processes. Furthermore, by employing Newtonian frameworks, it is postulated that there are absolute measures of time denoted as t_{ts} and t_{ps} in their respective spaces. Similar to space, time is also related by a differential identity of the form $dt_{ts} = gdt_{ps}$, where g is assumed to be both spatially and temporally invariant and positive.

2.2 Projected transport equations

After the quantification of space scaling in mathematical form, the focus now shifts on the effect of scaling on physical processes. The trial space physics (where scaled experiments sits) is projected onto the physical space (real life structures) by means of transport equations. The details of transport equations can be found in [23]. A generic form of transport equation in trial space can be represented as [18]:

$$\frac{D^*}{D^*t_{ts}}\int_{\Omega^*_{ts}} \rho_{ts}\boldsymbol{\Psi}_{ts}dV^*_{ts} + \int_{\Gamma^*_{ts}} \rho_{ts}\boldsymbol{\Psi}_{ts}(\boldsymbol{v}_{ts} - \boldsymbol{v}^*_{ts})\cdot \boldsymbol{n}_{ts}d\Gamma^*_{ts} = -\int_{\Gamma^*_{ts}} \boldsymbol{J}^{\Psi}_{ts}\cdot\boldsymbol{n}_{ts}d\Gamma^*_{ts} + \int_{\Omega^*_{ts}} \rho_{ts}\boldsymbol{b}^{\Psi}_{ts}dV^*_{ts} \quad (1)$$

Where, ρ_{ts} is material density, $\boldsymbol{\Psi}_{ts}$ is physical field, $\boldsymbol{v}_{ts}$ is material velocity, $\boldsymbol{v}^*_{ts}$ is velocity field in control volume, $\boldsymbol{J}^{\Psi}_{ts}$ is boundary flux, $\boldsymbol{b}^{\Psi}_{ts}$ is source term, dV^*_{ts} is elemental volume, $d\Gamma^*_{ts}$ is elemental surface area vector and $\boldsymbol{n}_{ts}$ represents the unit normal to the boundary Γ^*_{ts} of the control volume Ω^*_{ts}.

The Eq. (1) can be projected onto physical space by substituting $dV^*_{ts} = \beta^3 dV^*_{ps}$, $d\Gamma^*_{ts} = \beta^2 d\Gamma^*_{ps}$, $dt_{ts} = gdt_{ps}$. Multiplying the whole equation by g and scalar for transport equation for field Ψ in zeroth-order theory (α^{Ψ}_0) will lead to transport equation:

$$\begin{aligned}\alpha^{\Psi}_0 T^{\Psi}_0(\beta) = {} & \frac{D^*}{D^*t_{ps}}\int_{\Omega^*_{ps}} \alpha^{\Psi}_0\rho_{ts}\beta^3\boldsymbol{\Psi}_{ts}dV^*_{ps} \\ & + \int_{\Gamma^*_{ps}} \alpha^{\Psi}_0\rho_{ts}\beta^3\boldsymbol{\Psi}_{ts}(\beta^{-1}g\boldsymbol{v}_{ts} - \beta^{-1}g\boldsymbol{v}^*_{ts}) \\ & \cdot\boldsymbol{n}_{ps}d\Gamma^*_{ps} + \int_{\Gamma^*_{ps}} \alpha^{\Psi}_0\beta^2 g\boldsymbol{J}^{\Psi}_{ts}\cdot\boldsymbol{n}_{ps}d\Gamma^*_{ps} \\ & - \int_{\Omega^*_{ps}} \alpha^{\Psi}_0\rho_{ts}\beta^3 g\boldsymbol{b}^{\Psi}_{ts}dV^*_{ps} = 0\end{aligned} \quad (2)$$

In the case of solid and fracture mechanics, transport equations for volume, mass, momentum, and movement are of prime interest. The velocity field is constrained by transport equation of volume. Stress tensor field and specific body force is constrained by transport equation of momentum. Similarly, displacement field is constrained by transport equation of movement. Density and material velocity are constrained by transport equation of mass. The transport euation for the displacement field is of keen interest in fracture studies as continuity equations and others are generally fixed. Eq. (2) is a general projection of trial space onto physical space. In regards with fracture mechanics, the transport equations are given as follows. Scaled transport equation for volume:

$$\begin{aligned}\alpha^1_0 T^1_0(\beta) = {} & \frac{D^*}{D^*t_{ps}}\int_{\Omega^*_{ps}} \alpha^1_0\beta^3 dV^*_{ps} - \\ & \int_{\Gamma^*_{ps}} \alpha^1_0\beta^3(\beta^{-1}gv_{ts}\cdot\boldsymbol{n}_{ps})d\Gamma^*_{ps} \\ & = 0\end{aligned} \quad (3)$$

Scaled transport equation for mass:

$$\alpha_0^{\rho} T_0^{\rho}(\beta) = \frac{D^*}{D^* t_{ps}} \int_{\Omega_{ps}^*} \alpha_0^{\rho} \rho_{ts} \beta^3 dV_{ps}^* + \int_{\Gamma_{ps}^*} \alpha_0^{\rho} \rho_{ts} \beta^3 (\beta^{-1} g \boldsymbol{v}_{ts} - \beta^{-1} g \boldsymbol{v}_{ts}^*) \cdot \boldsymbol{n}_{ps} d\Gamma_{ps}^* = 0 \quad (4)$$

Scaled transport equation for momentum:

$$\alpha_0^{v} T_0^{v}(\beta) = \frac{D^*}{D^* t_{ps}} \int_{\Omega_{ps}^*} [\alpha_0^{v} g^{-1} \beta \rho_{ts} \beta^3](\beta^{-1} g \boldsymbol{v}_{ts}) dV_{ps}^* + \int_{\Gamma_{ps}^*} [\alpha_0^{v} g^{-1} \beta \rho_{ts} \beta^3](\beta^{-1} g \boldsymbol{v}_{ts}) (\beta^{-1} g \boldsymbol{v}_{ts} - \beta^{-1} g \boldsymbol{v}_{ts}^*) \cdot \boldsymbol{n}_{ps} d\Gamma_{ps}^* + \int_{\Gamma_{ps}^*} \alpha_0^{v} \beta^2 g \boldsymbol{\sigma}_{ts} \cdot \boldsymbol{n}_{ps} d\Gamma_{ps}^* - \int_{\Omega_{ps}^*} \alpha_0^{v} \rho_{ts} \beta^3 g \boldsymbol{b}_{ts}^{v} dV_{ps}^* = 0 \quad (5)$$

Scaled transport equation for movement:

$$\alpha_0^{u} T_0^{u}(\beta) = \frac{D^*}{D^* t_{ps}} \int_{\Omega_{ps}^*} [\alpha_0^{u} \beta \rho_{ts} \beta^3](\beta^{-1} \boldsymbol{u}_{ts}) dV_{ps}^* + \int_{\Gamma_{ps}^*} [\alpha_0^{u} \beta \rho_{ts} \beta^3](\beta^{-1} \boldsymbol{u}_{ts}) (\beta^{-1} g \boldsymbol{v}_{ts} - \beta^{-1} g \boldsymbol{v}_{ts}^*) \cdot \boldsymbol{n}_{ps} d\Gamma_{ps}^* - \int_{\Omega_{ps}^*} \alpha_0^{u} \beta \rho_{ts} \beta^3 (\beta^{-1} g \boldsymbol{v}_{ts}) dV_{ps}^* = 0 \quad (6)$$

Here, u denotes the displacement field. The purpose of α_0^{Ψ} term in Eq. (3), (4), (5), (6) is to eliminate β terms and $v_{ts}^* = \beta g^{-1} v_{ps}^*$ and $\alpha_0^1 = \beta^{-3}$ are essential conditions to satisfy zeroth order finite similitude thoery [19].

2.3 First-order finite similitude theory

The fact that the finite-similitude formulation is not constrained to one particular invariance is its primary advantage over dimensional analysis. A simple assumption is that the physics of the trial spaces do not change with scale; theoretically, this can be represented by the identity:

$$\frac{d}{d\beta}(\alpha_0^{\Psi} T_0^{\Psi}) \equiv 0 \quad (7)$$

Which when satisfied is termed as zeroth-order finite similitude. More details on this can be found in [23]. Here, symbol '$\equiv$' implies that derivative is identically zero. The notion of kth-order finite similitude is defined as the minimum derivative that fulfils the conditions:

$$T_{k+1}^{\Psi} = \frac{d}{d\beta}(\alpha_k^{\Psi} T_k^{\Psi}) \equiv 0 \quad (8)$$

$\forall \beta > 0$, with $\alpha_0^{\Psi} T_0^{\Psi}$ given by Eq. (2) where scalars α_k^{Ψ} are functions of β with $\alpha_k^{\Psi}(1) = 1$. Fracture analysis of scaled experimentation can be accurately done by using the two experiment theory; where, additional information can be obtained from the data [**?**]. Hence, first-order finite similitude theory has been shown to be adept for fracture studies [19] which can be written as:

$$T_2^{\Psi} = \frac{d}{d\beta}(\alpha_1^{\Psi} T_1^{\Psi}) = \frac{d}{d\beta}\left(\alpha_1^{\Psi} \frac{d}{d\beta}(\alpha_0^{\Psi} T_0^{\Psi})\right) \equiv 0 \quad (9)$$

The identities relevant to fracture mechanics and fatigue are derived by integrating eqn. 9 for each transport equation, and are as follows:

$$\boldsymbol{v}_{ps} = \beta_1^{-1} g_1 \boldsymbol{v}_{ts}(\beta_1) + R_1^{\rho} \quad (\beta_1^{-1} g_1 \boldsymbol{v}_{ts}(\beta_1) - \beta_2^{-1} g_2 \boldsymbol{v}_{ts}(\beta_2)) \quad (10)$$

$$\boldsymbol{v}_{ps} = \beta_1^{-1} g_1 \boldsymbol{v}_{ts}(\beta_1) + R_1^{v} \quad (\beta_1^{-1} g_1 \boldsymbol{v}_{ts}(\beta_1) - \beta_2^{-1} g_2 \boldsymbol{v}_{ts}(\beta_2)) \quad (11)$$

$$\boldsymbol{\sigma}_{ps} = \alpha_{01}^{v} g_1 \beta_1^2 \boldsymbol{\sigma}_{ts}(\beta_1) + R_1^{v} \quad (\alpha_{01}^{v} g_1 \beta_1^2 \boldsymbol{\sigma}_{ts}(\beta_1) - \alpha_{02}^{v} g_2 \beta_2^2 \boldsymbol{\sigma}_{ts}(\beta_2)) \quad (12)$$

$$\boldsymbol{b}_{ps}^{v} = g_1^2 \beta_1^{-1} \boldsymbol{b}_{ts}^{v}(\beta_1) + R_1^{v} \quad (g_1^2 \beta_1^{-1} \boldsymbol{b}_{ts}^{v}(\beta_1) - g_2^2 \beta_2^{-1} \boldsymbol{b}_{ts}^{v}(\beta_2)) \quad (13)$$

$$\boldsymbol{u}_{ps} = \beta_1^{-1} \boldsymbol{u}_{ts}(\beta_1) + R_1^{u} \quad (\beta_1^{-1} \boldsymbol{u}_{ts}(\beta_1) - \beta_2^{-1} \boldsymbol{u}_{ts}(\beta_2)) \quad (14)$$

$$\boldsymbol{v}_{ps} = \beta_1^{-1} g_1 \boldsymbol{v}_{ts}(\beta_1) + R_1^{u} \quad (\beta_1^{-1} g_1 \boldsymbol{v}_{ts}(\beta_1) - \beta_2^{-1} g_2 \boldsymbol{v}_{ts}(\beta_2)) \quad (15)$$

where, for consistent velocity it is necessary that $R_1 = R_1^{\rho} = R_1^{u} = R_1^{v}$ and it is inherently assumed that zeroth-order conditions apply.

2.4 Scale invariance in fracture mechanics

The stress field under scaling is the first thing to take into account, and it is argued that each of the scaled fracture specimens can be expected to have almost identical stress fields local to a crack tip. Due to this criterion, the theory should be able to account for the scale invariance, which reduces Eq. (12) to:

$$1 = \alpha_{01}^{v} g_1 \beta_1^2 + R_1(\alpha_{01}^{v} g_1 \beta_1^2 - \alpha_{02}^{v} g_2 \beta_2^2) \quad (16)$$

In differential terms, $\alpha_1^v(\alpha_0^v g \beta_2)$ is constant, where "constant" implies independent of β. It implies that fracture process zone can also be taken into account using this equation where it changes in the similar form. The fixing of displacement (separation in cohesive elements), i.e., $\boldsymbol{u}_{ps} = \boldsymbol{u}_{ts1} = \boldsymbol{u}_{ts2}$, which when applied to Eq. (14), provides another desirable scale invariance as:

$$1 = \beta_1^{-1} + R_1(\beta_1^{-1} - \beta_2^{-1}) \quad (17)$$

Further information on this topic can be explored in the scholarly work of Davey and Darvizeh [23], wherein they analyse the utilisation of transport equations in the context of fracture. Another important point of consideration is strain which can be written as:

$$\begin{aligned} \boldsymbol{\epsilon}_{ps} = \alpha_{01}^{v} g_1 \beta_1^2 \boldsymbol{\epsilon}_{ts1} + R_1(\alpha_{01}^{v} g_1 \beta_1^2 \boldsymbol{\epsilon}_{ts1} \\ - \alpha_{02}^{v} g_2 \beta_2^2 \boldsymbol{\epsilon}_{ts2}) \end{aligned} \quad (18)$$

This condition states that $\alpha_{01}^{v} g_1 \beta_1^2 = \alpha_{02}^{v} g_2 \beta_2^2 = 1$. It is important to note that g_1 and g_2 do not have any significance in a quasistatic analysis. Hence, the two experiment theory has freedom limited in the selection of scales β_1 and β_2.

3 DETERMINATION OF STRESS INTENSITY FACTOR USING TWO EXPERIMENT THEORY

Finite similitude theory has been used to estimate the stress intensity factor of a three-point bending specimens using two trial spaces. The trial spaces are combined in such a way that it can accurately estimate the value of larger physical space. The stress intensity factor for physical space can be defined as [19]:

$$\begin{aligned} K_{Ips} = \alpha_{01}^{v} g_1 \beta_1^{3/2} K_{Its1} + R_1(\alpha_{01}^{v} g_1 \beta_1^{3/2} K_{Its1} \\ - \alpha_{02}^{v} g_2 \beta_2^{3/2} K_{Its2}) \end{aligned} \quad (19)$$

Here, K_{Ips} is stress intensity factor for physical space. K_{Its1} and K_{Its2} are stress intensity factors for trial spaces 1 and 2 respectively. α, g, and β are the scaling factors. Further details on these can be found in [20].

Series of geometrically similar beams have been chosen for the present study from the existing literature [24]. The details of the beam specimen has been given in Table 1. The beams are of constant thickness of 50 mm with Young's modulus of 27000 MPa and Poisson's ratio 0.19. For the present study, medium and small beams are treated as trial spaces, ts1 and ts2, respectively. A virtual model for physical space has been constructed using these two trial spaces and the result has been matched with the large beam specimen; latter acting as physical space.

Table 1: Specimen dimensions of all beams [24]

Specimen	Span (S) (mm)	Length (L) (mm)	Depth (D) (mm)	Notch size (a_0) (mm)
Small(ts2)	200	300	50	10
Medium(ts1)	400	550	100	20
Large(ps)	800	1000	200	40

Values for the scaling factors mentioned in Eq. (19) are calculated for the present beam specimens, as $\alpha_{01}^{v} g_1 = \beta_1^{-2}$ and $\alpha_{02}^{v} g_1 = \beta_2^{-2}$ and presented in Table 2.

Table 2: Values of scaling factors for virtual model

Model	β_1	β_2	$\alpha_{01}^{v} g_1$	$\alpha_{02}^{v} g_1$	R_1
1	0.5	0.25	4	16	0.5

Using these factors, the applied loads for the scaled ts1 and ts2 models are calculated using peak load of physical model (ps) as [20]:

$$\begin{aligned} F_{ts1} = F_{ps}/\alpha_{01}^{v} g_1 = 1007.5N \\ F_{ts2} = F_{ps}/\alpha_{02}^{v} g_1 = 251.8N \end{aligned} \quad (20)$$

The stress intensity factor value for full scale model or physical model is estimated from the combination of trial models under the scaled loading using Eq. (19). In the following section, numerical model is presented for the used beam specimens.

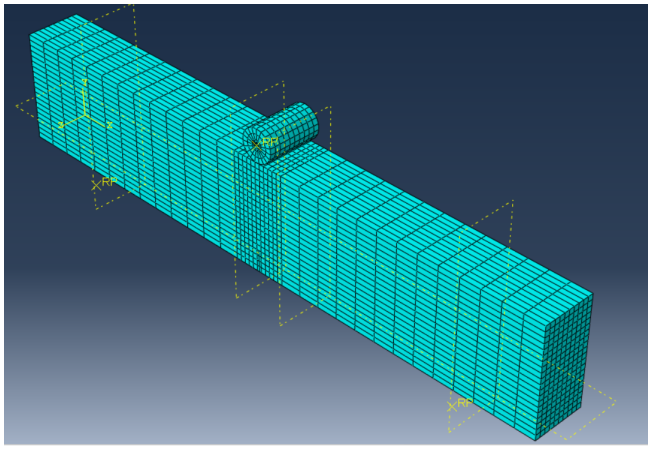

Figure 1: Mesh details of medium specimen

3.1 Numerical analysis

Prior to the application of any scaling rules, it is crucial to validate the numerical results in order to ascertain the accuracy of the numerical modelling and its alignment with existing published research. For this purpose, the crack growth in all three beams specimens is simulated using XFEM cohesive zone model in ABAQUS software. The XFEM fracture growth is determined by the linear elastic traction-separation model, damage initiation criteria, and damage evolution laws. In this study, the maximum principal stress is used in the damage initiation criteria [25], which determines the direction of initiation and propagation of crack. According to the maximum principal stress theory, material failure happens when the principal stress reaches its maximum value and the yield criteria is met. Damage evolution is applied in accordance with the descending linear portion of the bilinear traction-separation law, which represents the behaviour of material softening and stiffness degradation. The input of damage evolution is the fracture energy of the material, which represents the resistance to the extension of crack. The structured mesh with 8-node-linear brick element (C3D8R) is used for all specimens. The meshing for medium specimen is shown in Fig. 1 and the deformed physical model along with cracking profile is presented in Fig. 2.

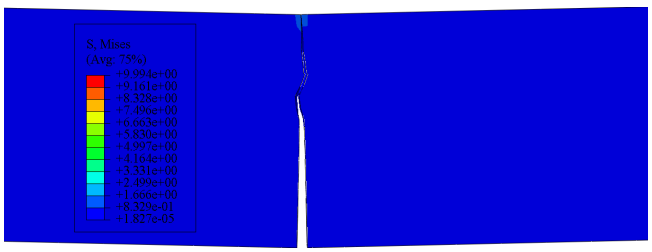

Figure 2: Cracking profile of medium beam specimen obtained from Abaqus

Another model for all three specimens have been prepared in ABAQUS to estimate the stress intensity factor at crack tip using contour integral method. The Von Mises stresses for these specimens are presented in Fig. 3, 4, 5.

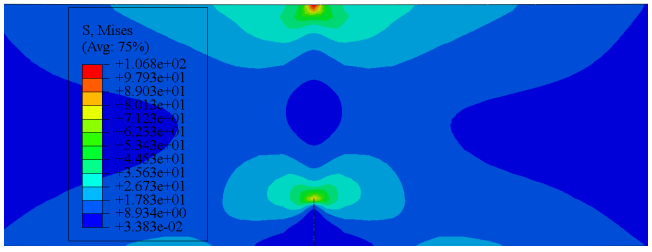

Figure 3: Von Mises stress distribution at the crack tip for large specimen

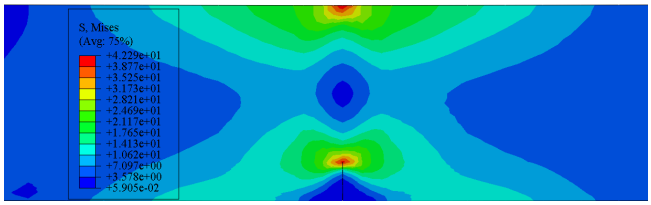

Figure 4: Von Mises stress distribution at the crack tip for medium specimen

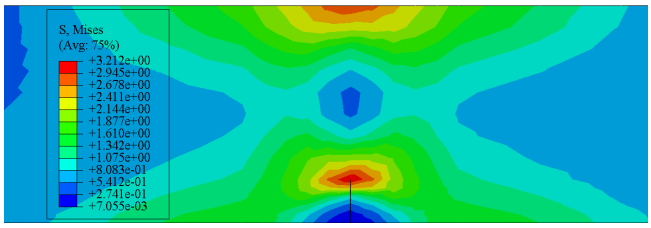

Figure 5: Von Mises stress distribution at the crack tip for small specimen

4 VALIDATION OF MODEL

The crack mouth opening displacement (CMOD) has been calculated from the deformed model along the crack propagation using XFEM. The load-CMOD curves are then plotted for all the specimens and compared with the experimental results. Fig. 6, 7, 8 shows the load-CMOD plots for large, medium and small specimens respectively. From the plots, it can be observed that a good aggrement is found with the experimental data. The calculated stress intensity factor values medium (ts1), small (ts2), and large (ps) has been reported in the Table 3. The virtual model made using combination of ts1 and ts2 has the K_I value of 268.8 MPa·$mm^{0.5}$, which is almost equal to the stress intensity factor of physical model. Thus, it can be inferred that the aforementioned finite similitude theory can be used for fracture studies of concrete.

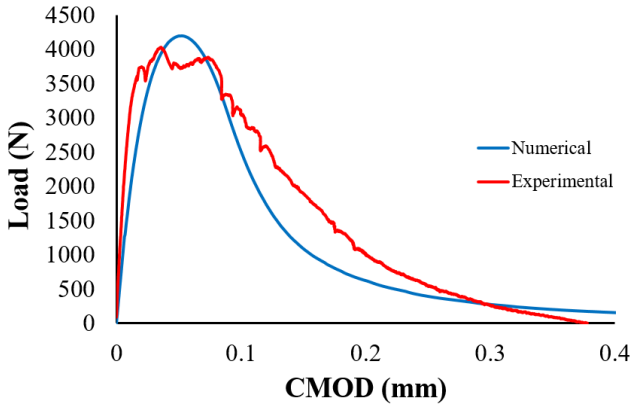

Figure 6: Comparison of Load-CMOD curves for large specimen

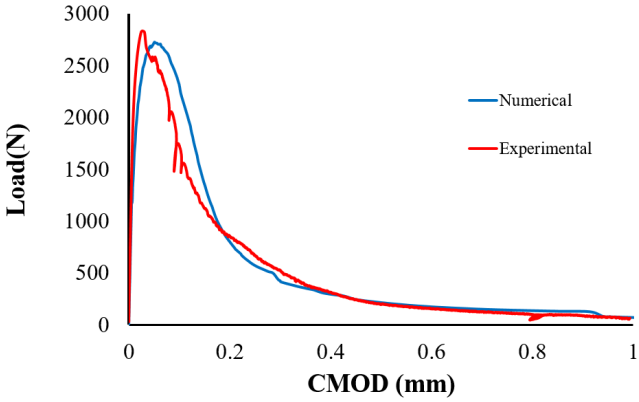

Figure 7: Comparison of Load-CMOD curves for medium specimen

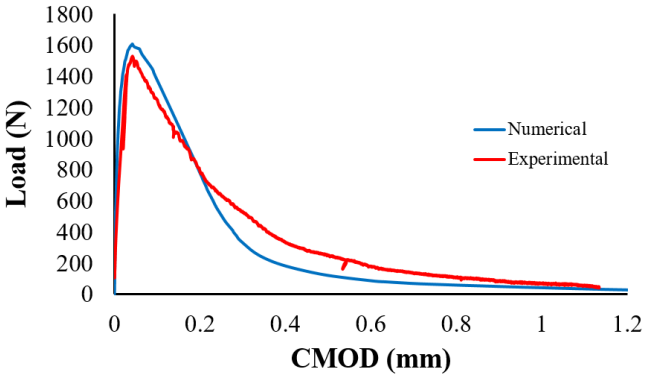

Figure 8: Comparison of Load-CMOD curves for small specimen

Table 3: Values of stress intensity factor for different models

Model	K_I (MPa.$mm^{0.5}$)
ts1	131.51
ts2	10.17
virtual	268.8
ps	266

5 CONCLUSIONS

This study investigates a novel framework for fracture mechanics of concrete based on the first-order finite similitude rule derived from finite similitude theory. The concept of first-order finite similitude combines data collected at two different scales in order to accurately replicate phenomena at the larger scale. The study involved an investigation of prior experimental data available in open literature pertaining to plain concrete. It was shown that, despite the existence of a geometric size effect, it is feasible to extrapolate the behaviour observed in full-scale model based on the outcomes of two scaled tests. The stress intensity factor in three-point bend notched concrete specimen is evaluated using the concepts of first order finite similitude theory. The study is validated using numerical results obtained from ABAQUS and a good agreement is found between them. The study can be further explored to define other fracture parameters and size effect in concrete structures under the action of cyclic loading.

REFERENCES

[1] Hossdorf, H. 1974. *Model analysis of structures*, Van Nostrand Reinhold Company, New York, USA.

[2] Galileo, G., Weston, J. 1730. *Mathematical Discourses concerning Two new sciences relating to Mechanical and local motion: in four dialogues*, John Hooke, London.

[3] Atkins, A. G. 1999. Scaling laws for elastoplastic fracture. *International journal of fracture* **95**:51–66.

[4] Bažant, Z.P., Chen, E. P. 1997. Scaling of structural failure. *Appl. Mech. Rev.* **50(10)**:593–627.

[5] Mazzariol, L. M., Oshiro, R. E., & Alves, M. 2016. A method to represent impacted structures using scaled models made of different materials. *International Journal of Impact Engineering* **90**:81–94.

[6] Neuberger, A., Peles, S., & Rittel, D. 2007. Scaling the response of circular plates subjected to large and close-range spherical explosions. Part I: Air-blast loading. *International Journal of Impact Engineering* **34(5)**:859–873.

[7] Grossmann, S., Lohse, D. 2020. Scaling in thermal convection: a unifying theory. *Journal of Fluid Mechanics* **407**:27–56.

[8] Moës, N., Dolbow, J., & Belytschko, T. 1999. A finite element method for crack growth without remeshing. *International Journal for Numerical Methods in Engineering* **46(1)**:131–150.

[9] Abaqus, G. 2011. *Dassault Systemes Simulia Corporation, Providence*, RI, USA. (3).

[10] Weibull, W. 1951. A statistical distribution function of wide applicability. *Journal of Applied Mechanics* Vol **18**.

[11] Bažant, Z.P., Novak, D. 2000. Energetic-statistical size effect in quasibrittle failure at crack initiation. *ACI Materials Journal* **97(3)**:381–392.

[12] Bažant, Z.P. 1984. Size effect in blunt fracture: concrete, rock, metal. *Journal of Engineering Mechanics* **110(4)**:518–535.

[13] Bhowmik, S., & Ray, S. 2016. Effects of fracture process zone on fatigue crack growth in concrete, *Proceedings of 9^{th} International Conference on Fracture Mechanics of Concrete and Concrete Structures*.

[14] Bhowmik, S., & Ray, S. 2018. An improved crack propagation model for plain concrete under fatigue loading. *Engineering Fracture Mechanics* **191**:365–382.

[15] Davey, K., Darvizeh, R., & Al-Tamimi, A. 2017. Scaled metal forming experiments: a transport equation approach. *International Journal of Solids and Structures* **125**:184–205.

[16] Goodier, J.N. & Thomson, W.T. 1944. *Applicability of similarity principles to structure models*, National Advisory Committee for Aeronautics, Washington, DC, (Report No. CR-4068).

[17] Goodier, J.N. 1950. *Dimensional Analysis*, Van Wiley, New York. USA.

[18] Davey, K., Darvizeh, R., & Zhang, J. 2021. Finite similitude in fracture mechanics. *Engineering Fracture Mechanics* **245**:107–573.

[19] Davey, K., Zhang, J., & Darvizeh, R. 2022. Fracture mechanics: A two-experiment theory. *Engineering Fracture Mechanics* **271**:108–618.

[20] Davey, K., Darvizeh, R., Akhigbe-Midu, O., & Sadeghi, H. 2022. Scaled cohesive zone models for fatigue crack propagation. *International Journal of Solids and Structures* **256**:111–956.

[21] Davey, K., Sadeghi, H., & Darvizeh, R. 2023. The theory of scaling. *Continuum Mechanics and Thermodynamics* **35(2)**:471–496.

[22] Davey, K., Akhigbe-Midu, O., Darvizeh, R., & Sadeghi, H. 2023. Scaled empirical fatigue laws. *Engineering Fracture Mechanics* **284**:109–258.

[23] Davey, K., & Darvizeh, R. 2016. Neglected transport equations: extended Rankine–Hugoniot conditions and J-integrals for fracture. *Continuum Mechanics and Thermodynamics* **28**:1525–1552.

[24] Bhowmik, S., & Ray, S. 2019. An experimental approach for characterization of fracture process zone in concrete. *Engineering Fracture Mechanics* **211**:401–419.

[25] Hearn, E.J. 1997. *Theories of Elastic Failure, Mechanics of materials. 1, An introduction of the mechanics of elastic and plastic deformation of solids and structural materials*, Oxford: Butterworth-Heinemann (1, 1997, 401-429 pp.).